ChemComm

COMMUNICATION

View Article Online
View Journal | View Issue

Cite this: *Chem. Commun.*, 2018, **54**, 13698

Received 9th October 2018,
Accepted 12th November 2018

DOI: 10.1039/c8cc08061e

rsc.li/chemcomm

A ruthenium(II) complex–cyanine energy transfer scaffold based luminescence probe for ratiometric detection and imaging of mitochondrial peroxynitrite†

Wenzhu Zhang,*[a] Yi Liu,[a] Quankun Gao,[a] Chaolong Liu,[a] Bo Song,[a] Run Zhang*[b] and Jingli Yuan*[a]

A novel ruthenium(II) complex–cyanine energy transfer scaffold has been established for the development of a ratiometric luminescence probe for ONOO$^-$ detection. The probe, Ru–Cy5, is localized in mitochondria of live cells, allowing ratiometric sensing and imaging of ONOO$^-$ therein.

As a member of reactive nitrogen species (RNS), peroxynitrite (ONOO$^-$) is endogenously generated by the diffusion-controlled reaction of endogenous nitric oxide (NO) and superoxide ($O_2^{\bullet -}$) mainly in mitochondria.[1] In living organisms, ONOO$^-$ at a reasonable concentration acts as a signalling transduction molecule to modulate a series of cellular functions, such as selective nitration of tyrosine residues.[2] On the other hand, an elevated level of ONOO$^-$ can directly oxidize or decompose lipids, proteins, and nucleic acids, leading to the apoptosis and death of cells.[2] Growing evidence has established that the level of ONOO$^-$ is highly correlated with the progress of various diseases and disorders, such as cardiovascular and metabolic diseases, shock, arteriosclerosis, neurodegenerative diseases and even cancers.[3] Therefore, an effective method for ONOO$^-$ detection is required that might benefit disease early diagnosis and treatment monitoring.

Towards this end, the development of molecular probes that are capable of sensing and imaging ONOO$^-$ has attracted considerable attention due to the advantages of high sensitivity, selectivity, and simplicity in data collection of sensing technology.[4–7] In the past few years, a number of probes have been engineered, allowing ONOO$^-$ detection to be performed by recording their emission intensity changes during the sensing process.[8–16] In comparison with the intensity on/off approach,[17–20] ratiometric probes that have a self-calibration of external interference on emission intensity are desirable for effective detection of ONOO$^-$ in mitochondria of live cells.[21–23]

The ratiometric changes in luminescence intensities at two emission wavelengths mainly arise from the factor of Förster resonance energy transfer (FRET) where generally organic dyes act as energy donors and acceptors. Energy transfer (ET) scaffolds established by exploiting luminescent metal complexes, especially ruthenium(II) complexes, are scarcely reported,[24,25] but such a scaffold is important due to the abundant photophysics and photochemistry properties of these luminophores, such as strong visible absorptions and emissions, large Stokes shifts, and good water solubility.[26–33] Furthermore, previous research of metal complex probes is mainly focused on the modulation of their excited states through photoinduced electron transfer (PET) and intramolecular charge transfer (ICT), leaving the ET scaffold strategy yet to be well demonstrated.

In this contribution, we report a Ru(II) complex–cyanine based ET scaffold and the development of a luminescence probe for ratiometric detection of ONOO$^-$. Based on this ET system, the ratiometric luminescence probe, **Ru–Cy5**, was engineered by employing a Ru(II) complex as the energy donor and Cy5 as the energy acceptor. The absorption of Cy5 (λ_{abs} = 630 nm) is diminished due to the ONOO$^-$-mediated oxidative cleavage of the polymethine bridge (Scheme 1A).[22] The ET from the Ru(II) complex to Cy5 is thus significantly interrupted (Scheme 1B), leading to the decrease of Cy5 emission (λ_{em} = 660 nm) and the increase of Ru(II) emission (λ_{em} = 610 nm) for ratiometric (I_{610}/I_{660}) detection of ONOO$^-$. Furthermore, owing to the mitochondria targeting feature of Cy5 after cellular internalization,[20] **Ru–Cy5** is expected to be localized in mitochondria, to enable ONOO$^-$ in this organelle to be visualized (Scheme 1C) under a ratiometric mode. To the best of our knowledge, this is the first report on constructing a Ru(II) complex–Cy5 ET probe for ratiometric luminescent sensing and imaging of biomolecules.

To synthesize **Ru–Cy5**, a Cy5 derivative, compound **8**, was first synthesized (Scheme S1, ESI†). Then, **Ru–Cy5** was obtained

[a] *State Key Laboratory of Fine Chemicals, School of Chemistry, Dalian University of Technology, Dalian 116024, China. E-mail: wzhzhang@dlut.edu.cn, jlyuan@dlut.edu.cn*

[b] *Australian Institute for Bioengineering and Nanotechnology, The University of Queensland, St. Lucia, QLD 4072, Australia. E-mail: r.zhang@uq.edu.au*

† Electronic supplementary information (ESI) available: General information, experimental section, synthesis and characterisation of **Ru–Cy5**, spectrometric response of **Ru–Cy5** towards ONOO$^-$, and MTT assay. See DOI: 10.1039/c8cc08061e

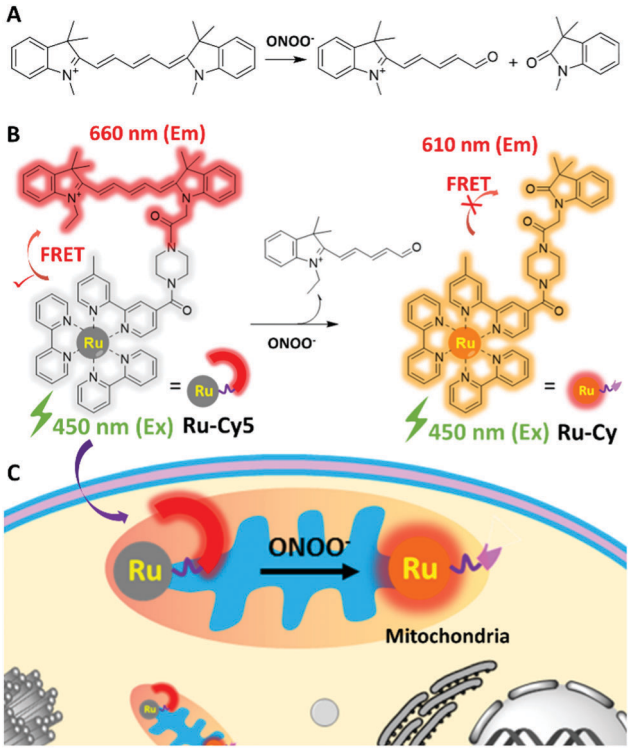

Scheme 1 (A) $ONOO^-$-mediated oxidative cleavage of the polymethine bridge of Cy5; (B) FRET scaffold of **Ru–Cy5** and its response mechanism to $ONOO^-$; (C) **Ru–Cy5** in the sensing and imaging of $ONOO^-$ in mitochondria of live cells.

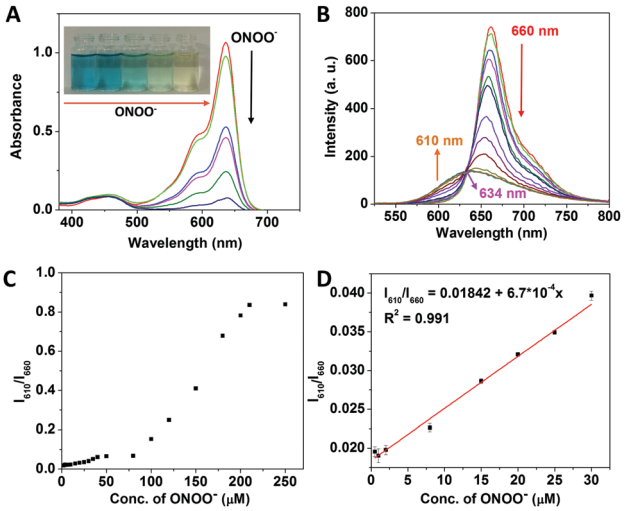

Fig. 1 (A) Absorption spectrum changes of **Ru–Cy5** (10 μM) in the presence of different concentrations of $ONOO^-$ (0, 30, 80, 100, 150 and 200 μM) in 25 mM PBS buffer of pH 7.4 (inset: color changes of the **Ru–Cy5** solution upon reaction with different concentrations of $ONOO^-$); (B) emission spectra (λ_{ex} = 450 nm) of **Ru–Cy5** (10 μM) upon reaction with different concentrations of $ONOO^-$ (0–220 μM); (C) the I_{610}/I_{660} ratio as a function of the $ONOO^-$ concentration; (D) calibration curve for the ratiometric luminescence detection of $ONOO^-$. The absorption and emission spectra were recorded after incubating **Ru–Cy5** with $ONOO^-$ for 30 min.

by reacting compound **8** with a Ru(II)-bipyridine complex derivative (complex **10**) that was synthesized through chloridization of the carboxyl acid in complex **9** (Scheme S1, ESI†). The chemical structures of all intermediates and **Ru–Cy5** were confirmed by NMR, ESI-MS, HRMS, and elemental analysis (Fig. S1–S17, ESI†). To validate the reaction mechanism of **Ru–Cy5** with $ONOO^-$, their reaction products were investigated by ESI-MS analysis. As shown in Fig. S18 (ESI†), the peak at *m*/*z* 632.20 was absent, and a new peak at *m*/*z* 448.70 that can be assigned to the species of $[\mathbf{Ru–Cy}]^{2+}$ was found, which confirmed the reaction of **Ru–Cy5** with $ONOO^-$, with the formation of $[\mathbf{Ru–Cy}]^{2+}$ as proposed in Scheme 1B.

In the absence and presence of $ONOO^-$, changes of UV-vis spectra in **Ru–Cy5** were initially examined in 25 mM PBS buffer of pH 7.4. As shown in Fig. 1A, the absorption spectrum of **Ru–Cy5** showed two intense absorption bands centred at 450 nm and 630 nm, which can be ascribed to the metal-to-ligand charge transfer (MLCT) absorption of the Ru(II) complex and the typical absorption of Cy5. Upon the reaction with $ONOO^-$, the absorption band at 630 nm was remarkably decreased due to the oxidization of Cy5, while no obvious changes at 450 nm were noticed, indicating the tolerance of the Ru(II) complex to $ONOO^-$. On increasing the concentration of $ONOO^-$, the color of the solution was clearly changed from blue to yellow (Fig. 1A inset). These facts indicate that **Ru–Cy5** can act as a "naked-eye" probe for $ONOO^-$ detection.

Significant changes in the emission spectrum of **Ru–Cy5** were also observed in the presence of different concentrations of $ONOO^-$ in 25 mM PBS buffer of pH 7.4 (Fig. 1B). Under excitation at 450 nm, **Ru–Cy5** exhibited a strong emission band centred at 660 nm, the characteristic emission of Cy5, which suggested the effective ET from the Ru(II) complex to the Cy5 moiety. In the presence of $ONOO^-$, owing to the oxidation of Cy5 and the corruption of ET (Scheme 1B), the emission band at 660 nm was remarkably decreased with the increase of the emission intensity at 610 nm. The ratio of the intensity at 610 nm to that at 660 nm (I_{610}/I_{660}) was found to be more than 46-fold enhanced in the presence of 200 μM $ONOO^-$ (Fig. 1C). Furthermore, the enhancement in the I_{610}/I_{660} ratio showed an excellent linear correlation to the concentration of $ONOO^-$ in the range from 0–30 μM. Based on the concentration corresponding to three standard deviations of the background signal, the detection limit ($3\sigma/k$) was calculated to be 0.28 μM. This result suggests that **Ru–Cy5** could be used as a ratiometric luminescence probe for highly sensitive quantification of $ONOO^-$ in aqueous media.

The specificity of **Ru–Cy5** for responding to $ONOO^-$ over other interfering species, including ROS, RNS, amino acids and metal ions, was investigated. As shown in Fig. 2A, more than 46-fold enhancement in the I_{610}/I_{660} ratio was noticed after **Ru–Cy5** was reacted with 20 equiv. of $ONOO^-$, while the reactions of **Ru–Cy5** with 100 equiv. of other species, including HOCl (20 equiv.), H_2O_2, $^{\bullet}OH$, $O_2^{\bullet-}$, $^1O_2$, NO, NO_2^-, HS^-, Cys, Hcy, GSH (5 mM), Ca^{2+}, Zn^{2+}, K^+, Na^+, Mg^{2+}, Fe^{2+} and Fe^{3+}, could not induce the change in the I_{610}/I_{660} ratio. These results reveal that the luminescence response of **Ru–Cy5** towards $ONOO^-$ is highly specific. The effect of pH on the ratiometric luminescence response of **Ru–Cy5** towards $ONOO^-$ was then evaluated in 25 mM PBS buffer with different pH values (pH 4–10). As shown in Fig. 2B, in the absence of $ONOO^-$, **Ru–Cy5** exhibited

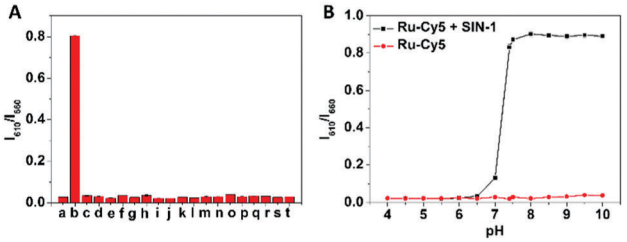

Fig. 2 (A) The I_{610}/I_{660} ratios of **Ru–Cy5** (10 μM) upon reactions with various ROS, RNS, amino acids and ions (a, control; b, $ONOO^-$; c, HOCl; d, NO_2^-; e, NO; f, HS^-; g, H_2O_2; h, $^{\bullet}OH$; i, $O_2^{\bullet-}$; j, $^1O_2$; k, Cys; l, Hcy; m, GSH (5 mM); n, Ca^{2+}; o, Zn^{2+}; p, K^+; q, Na^+; r, Mg^{2+}; s, Fe^{2+}; and t, Fe^{3+}) in 25 mM PBS buffer of pH 7.4. (B) Effects of pH on the I_{610}/I_{660} ratios of **Ru–Cy5** (10 μM) before and after the reaction with SIN-1 (200 μM). Excitation was performed at 450 nm.

small and stable I_{610}/I_{660} ratios in the pH range from 4 to 10. Upon reaction with 3-morpholinosydnonimine (SIN-1, a $ONOO^-$ donor, 200 μM), the I_{610}/I_{660} ratio remained low at pH below 6.5, and then rapidly increased to the maximum level at pH 7.5. Considering the weakly basic pH in mitochondria (pH ~8),[34,35] the above result indicates that **Ru–Cy5** is favorable to be used for the detection of $ONOO^-$ in the mitochondria of live cells.

Fig. S19 (ESI†) illustrated the time profile changes of the I_{610}/I_{660} ratio of **Ru–Cy5** in the absence and presence of 200 μM $ONOO^-$. The I_{610}/I_{660} ratio of **Ru–Cy5** kept at a low and stable value during the period of 25 min. However, upon the addition of $ONOO^-$, the I_{610}/I_{660} ratio was gradually increased, and reached a maximum after 20 min incubation, which reveals that the reaction between **Ru–Cy5** and $ONOO^-$ could be completed within 20 min. Upon the addition of $ONOO^-$, a good linearity between $ONOO^-$ concentration and the corresponding initial reaction rate is obtained (Fig. S20, ESI†). According to the reported methods,[36,37] the total reaction rate constant (k_{tot}) and reaction half-life time ($t_{1/2}$) were estimated to be 6.48×10^4 M^{-1} min^{-1} and 1.07×10^{-5} min, respectively.

On the basis of the above results, the feasibility of **Ru–Cy5** for sensing and imaging of mitochondrial $ONOO^-$ was evaluated. MTT assay showed that **Ru–Cy5** has low toxicity towards live cells. As shown in Fig. S21 (ESI†), no obvious changes in cell proliferation were noticed when HeLa cells were incubated with increased concentrations of **Ru–Cy5**. The cell viability remained more than 84% even after incubating HeLa cells with 50 μM of **Ru–Cy5** for 24 h, suggesting the low cytotoxicity of **Ru–Cy5** for loading live cells.

The distribution of **Ru–Cy5** in mitochondria of live cells was confirmed by colocalization analysis with a commercially available mitochondria labeling agent, MitoTracker™ Green FM. HeLa cells were incubated with 50 μM **Ru–Cy5** for 2 h, and then stained with MitoTracker™ Green FM for the colocalization analysis. As shown in Fig. 3, the mitochondrial distribution was supported by the synchronous luminescence signals in the linear region of interest across the cells. The excellent overlapping of red (**Ru–Cy5**) and green (MitoTracker™ Green FM) channels was observed. The Pearson's correlation coefficient (0.94) is close to 1, revealing the mitochondrial localization of the internalized **Ru–Cy5** molecules.

With the mitochondria-localization feature of **Ru–Cy5**, mitochondrial $ONOO^-$ in live cells was visualized *via* a ratiometric

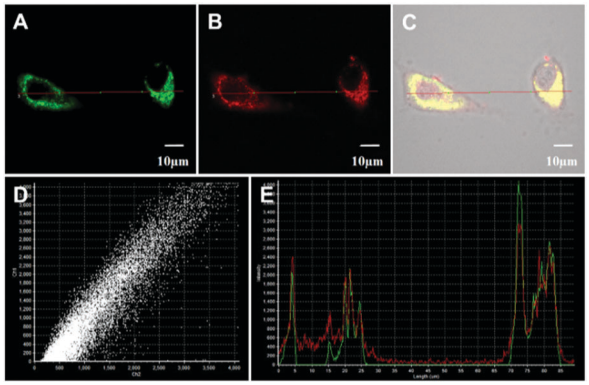

Fig. 3 Colocalization analysis of internalized **Ru–Cy5** and MitoTracker™ Green FM in HeLa cells. (A) Green channel of MitoTracker™ Green FM; (B) red channel of **Ru–Cy5**; (C) merged image of A, B, and a bright-field image; (D) intensity correlation plot of **Ru–Cy5** and MitoTracker™ Green FM; (E) intensity profiles of the linear regions of interest (ROIs) across HeLa cells. Excitation at 488 nm was used for both the red channel (640–680 nm) and the green channel (500–540 nm).

luminescence imaging approach. As shown in Fig. 4, under laser excitation at 488 nm, the control group of HeLa cells (incubated with 25 μM **Ru–Cy5** for 2 h only) showed a weak signal in the Ru(II) channel (590–630 nm) and an intense signal in the Cy5 channel (640–680 nm). After supplying with 500 μM SIN-1 for 30 min, significant decrease of the Cy5 channel signal and increase of the Ru(II) channel signal were observed, with a more than 7-fold change of the luminescence intensity ratio. These results demonstrated the feasibility of **Ru–Cy5** for the visualization of mitochondrial $ONOO^-$ in live cells under ratiometric mode.

In summary, a Ru(II) complex–cyanine energy transfer based luminescence probe, **Ru–Cy5**, has been developed for the ratiometric

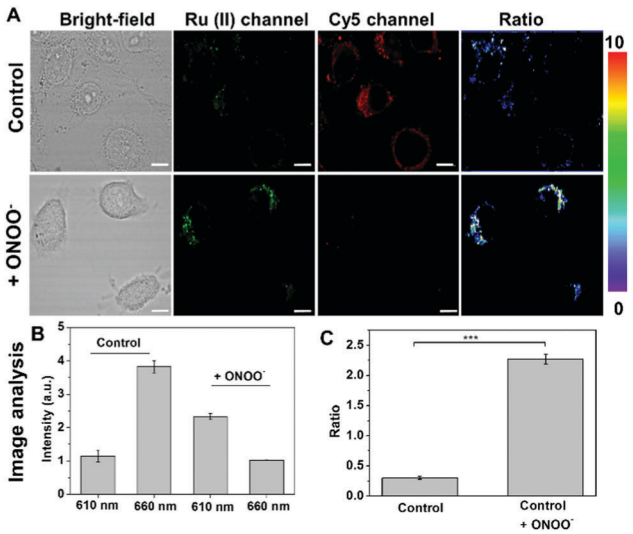

Fig. 4 Confocal luminescence images of $ONOO^-$ in HeLa cells using **Ru–Cy5** as a probe. (A) HeLa cells were incubated with **Ru–Cy5** (25 μM) for 2 h at 37 °C and then treated with 500 μM SIN-1 for 30 min (control group: HeLa cells were stained with **Ru–Cy5** only). Image analysis: luminescence intensity analysis (B) and changes of the luminescence intensity ratio (C). Scale bar: 10 μm.

detection of $ONOO^-$. This probe showed high response specificity and sensitivity to $ONOO^-$, as well as low cytotoxicity, good cell membrane permeability and mitochondria-localization feature, which enabled it to be successfully used for the ratiometric sensing and imaging of $ONOO^-$ in the mitochondria of live cells, to provide a useful tool for investigating the functions of $ONOO^-$ in live cells. In addition, the ET scaffold strategy described in this work also contributes to the future development of luminescent transition metal complex-based ratiometric probes.

We gratefully acknowledge the financial support from the National Natural Science Foundation of China (Grant No. 21475015, and 21775015), and Australian Research Council (DE170100092). The facilities and assistance of the Queensland Node of the Australian National Fabrication Facility (ANFF-Q), The University of Queensland, are also acknowledged.

Conflicts of interest

There are no conflicts to declare.

Notes and references

1 C. C. Winterbourn, *Nat. Chem. Biol.*, 2008, **4**, 278–286.
2 C. Szabó, H. Ischiropoulos and R. Radi, *Nat. Rev. Drug Discovery*, 2007, **6**, 662–680.
3 P. Pacher, J. S. Beckman and L. Liaudet, *Physiol. Rev.*, 2007, **87**, 315–424.
4 S. T. Manjare, Y. Kim and D. G. Churchill, *Acc. Chem. Res.*, 2014, **47**, 2985–2998.
5 R. Zhang, B. Song and J. Yuan, *TrAC-Trend Anal. Chem.*, 2018, **99**, 1–33.
6 X. Chen, X. Tian, I. Shin and J. Yoon, *Chem. Soc. Rev.*, 2011, **40**, 4783–4804.
7 M. Gao, F. Yu, C. Lv, J. Choo and L. Chen, *Chem. Soc. Rev.*, 2017, **46**, 2237–2271.
8 T. Yudhistira, S. V. Mulay, K. J. Lee, Y. Kim, H.-S. Park and D. G. Churchill, *Chem. – Asian J.*, 2017, **12**, 1927–1934.
9 D.-Y. Zhou, Y. Li, W.-L. Jiang, Y. Tian, J. Fei and C.-Y. Li, *Chem. Commun.*, 2018, **54**, 11590–11593.
10 D. Li, J. Cheng, C.-K. Wang, H. Ying, Y. Hu, F. Han and X. Li, *Chem. Commun.*, 2018, **54**, 8170–8173.
11 L. Wu, Y. Wang, M. Weber, L. Liu, A. C. Sedgwick, S. D. Bull, C. Huang and T. D. James, *Chem. Commun.*, 2018, **54**, 9953–9956.
12 H. Zhang, J. Liu, Y.-Q. Sun, Y. Huo, Y. Li, W. Liu, X. Wu, N. Zhu, Y. Shi and W. Guo, *Chem. Commun.*, 2015, **51**, 2721–2724.
13 J.-T. Hou, J. Yang, K. Li, Y.-X. Liao, K.-K. Yu, Y.-M. Xie and X.-Q. Yu, *Chem. Commun.*, 2014, **50**, 9947–9950.
14 W. Zhang, X. Wang, P. Li, H. Xiao, W. Zhang, H. Wang and B. Tang, *Anal. Chem.*, 2017, **89**, 6840–6845.
15 Q. Zhang, Z. Zhu, Y. Zheng, J. Cheng, N. Zhang, Y.-T. Long, J. Zheng, X. Qian and Y. Yang, *J. Am. Chem. Soc.*, 2012, **134**, 18479–18482.
16 F. Yu, P. Li, B. Wang and K. Han, *J. Am. Chem. Soc.*, 2013, **135**, 7674–7680.
17 X. Xie, F. Tang, G. Liu, Y. Li, X. Su, X. Jiao, X. Wang and B. Tang, *Anal. Chem.*, 2018, **90**, 11629–11635.
18 J. Li, C. S. Lim, G. Kim, H. M. Kim and J. Yoon, *Anal. Chem.*, 2017, **89**, 8496–8500.
19 D. Cheng, W. Xu, L. Yuan and X. Zhang, *Anal. Chem.*, 2017, **89**, 7693–7700.
20 D. Yang, H.-L. Wang, Z.-N. Sun, N.-W. Chung and J.-G. Shen, *J. Am. Chem. Soc.*, 2006, **128**, 6004–6005.
21 X. Zhou, Y. Kwon, G. Kim, J.-H. Ryu and J. Yoon, *Biosens. Bioelectron.*, 2015, **64**, 285–291.
22 X. Jia, Q. Chen, Y. Yang, Y. Tang, R. Wang, Y. Xu, W. Zhu and X. Qian, *J. Am. Chem. Soc.*, 2016, **138**, 10778–10781.
23 C. Song, Z. Ye, G. Wang, J. Yuan and Y. Guan, *Chem. – Eur. J.*, 2010, **16**, 6464–6472.
24 Q. Shao and B. Xing, *Chem. Commun.*, 2012, **48**, 1739–1741.
25 M.-J. Li, K. M.-C. Wong, C. Yi and V. W.-W. Yam, *Chem. – Eur. J.*, 2012, **18**, 8724–8730.
26 A. M.-H. Yip and K. K.-W. Lo, *Coord. Chem. Rev.*, 2018, **361**, 138–163.
27 E. Baggaley, M. R. Gill, N. H. Green, D. Turton, I. V. Sazanovich, S. W. Botchway, C. Smythe, J. W. Haycock, J. A. Weinstein and J. A. Thomas, *Angew. Chem., Int. Ed.*, 2014, **53**, 3367–3371.
28 M. R. Gill, J. Garcia-Lara, S. J. Foster, C. Smythe, G. Battaglia and J. A. Thomas, *Nat. Chem.*, 2009, **1**, 662–667.
29 G.-J. Yang, W. Wang, S. W. F. Mok, C. Wu, B. Y. K. Law, X.-M. Miao, K.-J. Wu, H.-J. Zhong, C.-Y. Wong, V. K. W. Wong, D.-L. Ma and C.-H. Leung, *Angew. Chem., Int. Ed.*, 2018, **57**, 13091–13095.
30 D.-L. Ma, L.-J. Liu, K.-H. Leung, Y.-T. Chen, H.-J. Zhong, D. S.-H. Chan, H.-M. D. Wang and C.-H. Leung, *Angew. Chem., Int. Ed.*, 2014, **53**, 9178–9182.
31 K. Y. Zhang, P. Gao, G. Sun, T. Zhang, X. Li, S. Liu, Q. Zhao, K. K.-W. Lo and W. Huang, *J. Am. Chem. Soc.*, 2018, **140**, 7827–7834.
32 Y. Chen, R. Guan, C. Zhang, J. Huang, L. Ji and H. Chao, *Coord. Chem. Rev.*, 2016, **310**, 16–40.
33 Z. Du, B. Song, W. Zhang, C. Duan, Y.-L. Wang, C. Liu, R. Zhang and J. Yuan, *Angew. Chem., Int. Ed.*, 2018, **57**, 3999–4004.
34 J. Llopis, J. M. McCaffery, A. Miyawaki, M. G. Farquhar and R. Y. Tsien, *Proc. Natl. Acad. Sci. U. S. A.*, 1998, **95**, 6803–6808.
35 M. F. C. Abad, G. Di Benedetto, P. J. Magalhães, L. Filippin and T. Pozzan, *J. Biol. Chem.*, 2004, **279**, 11521–11529.
36 B. Song, G. Wang, M. Tan and J. Yuan, *J. Am. Chem. Soc.*, 2006, **128**, 13442–13450.
37 R. Zhang, Z. Ye, G. Wang, W. Zhang and J. Yuan, *Chem. – Eur. J.*, 2010, **16**, 6884–6891.